

1-28-2014

Synthesis and Characterization of Zinc--Oxide/ Polystyrene Nanocomposite Thin Films

Christopher Krapu

Macalester College, ckrapu@gmail.com

Follow this and additional works at: <http://digitalcommons.macalester.edu/mjpa>

 Part of the [Astrophysics and Astronomy Commons](#), and the [Physics Commons](#)

Recommended Citation

Krapu, Christopher (2013) "Synthesis and Characterization of Zinc--Oxide/Polystyrene Nanocomposite Thin Films," *Macalester Journal of Physics and Astronomy*: Vol. 1: Iss. 1, Article 7.

Available at: <http://digitalcommons.macalester.edu/mjpa/vol1/iss1/7>

This Capstone is brought to you for free and open access by DigitalCommons@Macalester College. It has been accepted for inclusion in Macalester Journal of Physics and Astronomy by an authorized administrator of DigitalCommons@Macalester College. For more information, please contact scholarpub@macalester.edu.

Synthesis and Characterization of Zinc-Oxide/Polystyrene Nanocomposite Thin Films

Christopher Krapu

Macalester College

Abstract:

Ultra-thin films containing zinc oxide and polystyrene were prepared by sol-gel mixing and spincoating onto silicon substrate. Photoluminescent measurements were recorded following irradiation at 325 nm. We observed passivation of shallow defect states around 3.1 eV in the nanocomposite films as well as possible excitonic emission enhancement of the 3.3 eV bandgap via confinement. Time-resolved photoluminescence plots suggest a significant time dependence of emission intensity related to photodegradation of the polymer matrix.

Introduction

Researchers across the fields of electrical engineering, physics and chemistry have devoted much attention in recent years to the development and characterization of nanocomposite materials. Some of this interest is due to the qualitative change of the host material in response to the inclusion of filler nanoparticles. However, there still remains some uncertainty as to the change of the properties of the nanoparticles after inclusion into a larger composite system. The size-scale of nanoparticles—and in our case, semiconductor nanocrystals—used in these composites results in a special importance being attached to the surface defect states which deviate from the typical band gap structure of a bulk material and are a major part of the behavior of the nanoparticles. Previous studies [1] have focused on the properties of the composite whole as well as the bulk form of the composite. Motivation for these inquiries can be found in the manufacture of semiconductor devices using both bulk nanocomposite as well as thin-films. Polymeric coatings with nanofillers are still relatively new, however and the ultra-thin dimensions possible with various coating methods introduce yet another set of conditions in which to observe the varying properties of nanoparticles in the polymer matrix. Theorized applications of ZnO/polymer films include solar cells and UV-absorptive coatings. Significant amounts of research have been done on the pairing of zinc oxide-polymethyl-methacrylate (ZnO/PMMA) nanocomposites [1][2] in bulk and thin film forms; ZnO is a group II-VI semiconductor with morphologies that include the nanocrystals used in our composite as opposed to nanowires, nanobelts and other elongated growth morphologies more favored for study because of the preferential growth axes of ZnO crystals [3]. The photoluminescent behavior of zinc oxide-polystyrene (ZnO/PS) films should be expected to follow similar lines as ZnO/PMMA because of the closely-related polymer structure of both as well as a relatively small gap between the predicted near-band edge/deep level emission ratios for each. Previous research efforts have been directed towards these metal oxide/polymer composites and a few have been relevant to thin film studies, but none have used spin-coating as a method of production for

ultra-thin films containing polystyrene and zinc oxide nanocrystals. Since the focus of our study is primarily on the behavior of defect states near the crystal-polymer interface, the film thickness is a critical parameter for benchmarking the nanocomposite behavior. A salient feature of nanoparticles versus their macroscopic counterparts is a much higher surface-to-volume ratio leading to behavior predominantly derived from surface effects.

The ratio of near band edge (NBE) /deep level emission (DLE) intensity—a comparison of significance between the shallow defects versus deep defects—is computationally predicted to be roughly the same for ZnO/PMMA nanocomposites and ZnO/PS ones [4]. Deep level defects can result from oxygen vacancies or zinc interstitial defects in the ZnO lattice [4]. As the symmetry of the lattice structure is broken, the ZnO molecules have “dangling” bonds which then contribute to deep level emissions corresponding to a green wavelength of emitted photons (~520 nm) [5]. These defects negatively impact the performance of ZnO-based composites in applications such as photodetectors or UV-absorbent coatings, but encapsulation in bulk polymer has proven effective in mitigating these effects by passivating the unbonded ZnO nanoparticle surface with various bonds to the polymer [5].

Our analysis of charge dynamics in nanofilled polymer films involved both synthesis, using solution mixing and spincoating methods as well as characterization via photoluminescence (PL) and surface photovoltage/transient photovoltage (SPV) measurements. PL testing is useful in determining the primary emission peaks of the band-gap structure as it is altered by inclusion into a material. Zinc oxide nanoparticles—the primary focus of this experiment—can be described by a characteristic emission peak at 3.3 eV corresponding to the primary band-gap difference in electron energy levels as well as several smaller peaks corresponding to surface defects and other effects from the material. ZnO/PMMA composites prepared by bulk polymerization have been observed exhibiting significantly enhanced

excitonic emission features at room temperature [1] compared to pure ZnO. This suggests that the interface between ZnO and its polymer host affects the recombination behavior in the semiconductor.

Methodology

Various sources [1][2] have commented on the difficulty of achieving excellent dispersion of ZnO in PS or PMMA. Filler and host matrix tend to avoid mixing because of zinc oxide's hydrophilic nature contrasting with the hydrophobicity of polystyrene and many other commonly used polymers.

Creation of the thin film samples was performed using a sol-gel technique and deposition onto silicon wafers. Substrate preparation initially involved a modified Shiraki etch consisting of treatment with hydrofluoric acid followed by a standard RCA clean, deionized water rinse and ultrasonication for five minutes. Sample testing revealed that samples exhibited no significant deviation in surface purity from those which were cleaned with only the DI water and sonication. All samples which were tested were prepared without the Shiraki etch and RCA clean. The substrate materials were dried via spinning at >5000 RPM for 30 seconds. The silicon wafers were of Miller index (1,0,0) and were divided into rectangular pieces approximately 3-4 cm². The mixture for deposition was a combination of zinc oxide nanoparticles with a mean length scale of 20 nm purchased from Sigma Aldrich and a polystyrene (2800 MW)-toluene solution. A major difficulty in the production of the films was finding the correct range of polystyrene (PS) to use in a certain amount of toluene; various sources suggested a range of 3 percent PS by mass to as much as 15 or even 20[6]. We tested films produced through most of this range and observed that the sol-gel transition on the spin coater was nonuniform for solutions containing >9% PS. Nonuniformity was clearly visible from the interference patterns on the sample which suggested that the polymer solution was simply too viscous to evenly dry during spinning. For lower percentages, we were able to create thin films which exhibited uniform deposition as evidenced by their interference patterns. This behavior was in stark contrast to the "oil slick" patterns which we had found with

polymer-rich solutions. Because of the rectangular shape of the wafer piece [7] and the rotation of the spincoating machine, edge-effects from the spinning process were always a major detriment to the quality and uniformity of the films produced. Once the technique of producing the polystyrene films was mastered, zinc oxide nanoparticles (~20 nm average size from Sigma Aldrich) were mixed in successively larger amounts into various concentrations of a polystyrene-toluene solution. The surface properties of the ZnO nanocrystals led them to agglomerate in the solution, necessitating both heating and ultrasonication to achieve relatively uniform dispersion throughout the solution. The mixing procedure consisted of 1 hour of magnetic stirring at 30 degrees Celsius followed by 30 minutes in an ultrasonic bath. Initial batches were composed of parts ZnO and PS on the same order of magnitude but this was quickly realized to be far too much filler; the most uniform and high-quality thin films were produced with concentrations of ZnO which were ~5-20% of PS by mass. The final step in preparing the thin film samples was the deposition from solution onto substrate and spin-casting. Various RPM regimes on a SCS 6800NP spin coater were tested, and we found that a range from 1000-1500 RPM for 30 seconds produced the most uniform films of the desired thickness (<1 micron). Despite narrowing the range of parameters required for optimal film production, the majority of samples spun in all ranges were nonuniform; each deposition was done under fume hood in standard atmospheric conditions and airborne dust particles happened to settle and induce streaking during the spincoating process. Other defects included uneven deposition of solution onto substrate as well as agglomeration of ZnO nanoparticle clusters during the deposition process. However, after correcting for these errors with the previously mentioned processes we were able to obtain several films of high quality and uniform particle dispersion for a range of concentrations of ZnO. Further investigation was done with SEM measurements that confirmed excellent dispersion through a 1 micron length scale for these selected composite films.

Running concurrently with the fabrication of ZnO/PS thin films was the testing of the suitability of other solutions and mixtures for spincoating; our broader goal was to refine the experimental process and generalize it to produce many other combinations of materials. We found the procedure listed above to be satisfactory for producing films consisting of mixtures of barium titanate (BaTiO_3) along with PMMA. Moreover, an abbreviated process consisting of a cleaning cycle and spincoating with organic dyes was also able to produce thin films on a similar thickness scale.

Characterization of the thin film samples was performed by frequency-resolved and time-resolved photoluminescence (PL) testing as well as a few recorded runs measuring the surface photovoltage. The PL stimulation was achieved with a Helium-Cadmium 325 nm laser. Photoluminescence testing is useful for determining the energy levels available to electrons in a substance. Moreover, it is a contactless and—mostly—nondestructive testing method making it highly suitable for thin films. As we were interested mostly in the surface defect states of the ZnO after immersion in a polymer matrix, we focused on the wavelength range relevant to the energy levels of the defect states. A unique property of ZnO is that its excitonic binding energy is approximately 60meV and makes excitonic (band gap) recombination emissions appear at a UV wavelength. This feature is typically expected to interact with the band gap at 3.3 eV and lower the energy of this admission without altering defect bands occurring at photon energies of 3.1 and 2.4 eV [1].

Results and Discussion

Our base materials were tested as controls versus a ZnO/PS composite film (ZnO 5% of PS by mass). The PL testing measured intensity of emitted radiation versus wavelength at room temperature, running over wavelengths corresponding to emitted photon energies of 1.5-3.5 eV and is plotted in Figure 1. This range was determined from other studies of ZnO/polymer composites that found all relevant charge behavior to be contained within this range [1][2][3]. The bare nanopowder exhibited predicted spectra

including a broad deep-level defect emission (DLE) peak at approximately 2.4 eV. At the energy of 3.3 eV, the primary band-gap peak is merged with a shallow defect peak at 3.1 eV. Finding these emissive maxima was accomplished using Gaussian deconvolution. The nanopowder's (see Figure 2) spectrum appears to have a single large peak at 3.3 eV but best fit was achieved by accounting for the 3.1 eV NBE which provided an inflection point in the >3 eV distribution. No qualitatively significant peak broadening due to excitonic recombination was observed. A pure polystyrene film was similarly analyzed and plotted in Figure 2. A deconvolution with 4 peaks and an intensity maximum at ~2.35 eV provided the best fit. The polystyrene emissions were roughly one order of magnitude smaller than the ZnO nanoparticles.

Following initial runs of the bare nanoparticles and pure polymer films, we performed two consecutive frequency-resolved 40-minute PL tests (Figures 3, 4 and 5) on the composite film selected earlier. The first run shown in Figure 3 gave a spectrum with a significantly narrower distribution at 3.3 eV as well as a much more intense emission peak at 2.9 eV. The ZnO DLE at 2.4 eV was relatively unchanged in the first test. The shallow defect peak disappeared completely from the composite film fit. A deconvolution placing a single peak at 3.3 eV failed to accurately capture the spectral behavior in this region and we theorize this is the result of NBE/excitonic emissions. While excitonic behavior is negligible compared to thermal energy at room temperature for pure ZnO, several studies [1][2][4] observed enhanced excitonic emission due to ZnO inclusion in PMMA at room temperature and we theorize a similar mechanism is responsible for the broadening of the 3.3 eV peak.

The 2.9 eV maximum appears to result from the inclusion of PS though its intensity is increased by a factor of 3 from the pure PS film. We immediately ran another test of the same sample approximately half an hour after the first. The second spectrum shown in Figure 4 contained features which were qualitatively located at similar emission energy peaks, but with an enormous change in intensity. Most

significantly, the emission peak at 2.4 eV which was a feature in both the PS film and the bare ZnO nanopowders showed a nearly 5x increase in intensity while the ~2.9 eV peak which also figured prominently in the PS film jumped by a factor of 8. See Figure 5 for a relative comparison. The ZnO bandgap peak experienced a 30 percent increase in magnitude and the shallow defect peak was absent. A time-resolved PL plot (Figure 6) of the intensity of emitted radiation for the 3.3 eV and 2.9 eV peaks appeared to be an exponential function of time for the range 1-500s. During irradiation, a small amount of visible light was observed to be emanating from the composite film. In the post-test inspection, we expected to find obvious damage resulting from thermal warping and distortion of the films but they appeared to be unchanged. A purely thermal mechanism for this radiation is judged to be unlikely; nanoparticle inclusion is thought to improve thermal stability of the polymer matrix [8]. Random lasing has been observed in bulk materials using ZnO nanoparticles [9], but we view this as extremely unlikely in our sample because the film is nearly 2-dimensional and does not have the bulk volume allowing for random lasing paths. A more reasonable explanation is the photodegradation of the PS led to an abundance of product molecules with energy states overlapping the broad defect level. By itself, this explanation would fail to explain for the increase in the 3.3 eV bandgap peak. We propose a mechanism based on confinement; the polymer matrix could be expected to increase the quantum confinement effect on the bulk excitons, increasing their binding energy and thus allow them to contribute significantly to the NBE spectral behavior. PL from 20nm ZnO nanocrystals is thought to be due to recombination of donor-bound excitons [10]. Unfortunately, we did not measure at a sufficient resolution to be able to adequately distinguish excitonic contributions to this peak.

Virtually all possible mechanisms for the increase in luminescent intensity are tied to irreversible effects in the film layer; we can safely conclude that this degradation drastically reduces the suitability of ZnO/PS films for most applications; the susceptibility of our sample to near UV radiation precludes its

use in UV absorption—a primary use of ZnO-based nanomaterials. This degradation has not been observed in the cases of ZnO/PMMA [1][2] and so distinguishes the two cases.

Conclusion

We have found that production of uniform, ultra thin film metal-oxide/polymer composites can be achieved with a combination of sol-gel and spincoating methods. The resulting nanocomposite combination of zinc oxide and polystyrene bears many qualitative similarities to composites utilizing other polymer hosts including a passivation of shallow surface states and possible enhancement of donor-bound excitons in its photoluminescent response. However, we observed a major time-dependence of measured intensity during irradiation. This response is likely tied to a destructive process in the film that suggests an extreme vulnerability to UV radiation. Since many of the most prominent uses of semiconductor-containing thin films are relevant to light absorption—i.e. solar cells or anti-UV coatings—these point to a sharply reduced utility of ZnO/PS thin films. Further work remains to be done on various other thin-film combinations from a spincoating fabrication.

Acknowledgements

The author would like to thank Dr. Yuri Strzhemechny for advising this project, as well as Sebastian Requena and Srijan Lacoul for indispensable advice, insight and help in performing this experiment. This work was supported by Texas Christian University and the National Science Foundation's Research Experience for Undergraduates program (Grant #0851558).

References

- [1] Paramo *et al.*, J. Appl. Phys. **108**, 023517 (2010)
- [2] Liu *et al.*, Appl. Phys. Lett. **96** 023111 (2010)
- [3] Wang, L.W., J. Phys. Condens. Matter **16** 829 (2004)
- [4] Richters *et al.*, Appl. Phys. Lett. **92** 011103 (2008)
- [5] L. Qin, C. Shing, S. Sawyer, P. Dutta, Opt. Materials **33** 359 (2011)
- [6] Lock *et al.* Naval Research Laboratory NRL/MR/6750--08-9092
- [7] W.W. Flack, D.S. Soong, A.T. Bell, D.W. Hess, J. Appl. Phys. **56** 1199 (1984)
- [8] E.Tang, G. Cheng, X. Ma, Powder Tech., **161** 209 (2006)
- [9] Son *et al.*, Nanotechnology **20** 195203 (2009)
- [10] V.A Fonoberov, K.A. Alim, A.A. Balandin, Phys. Rev. B. **73** 165317 (2006)

Figure Captions

FIG. 1. Wide-range photoluminescence plot of polystyrene spincast onto silicon substrate. Light green curves are deconvoluted Gaussian distributions.

FIG. 2. PL plot of pure zinc oxide nanopowders (20 nm size)

FIG. 3. Initial testing of nanocomposite film. Note magnitude of dependent variable axis in comparison to figure 4.

FIG. 4. Second test of same film. Massive jump in intensity compared to first run.

FIG. 5. Comparative plot of ZnO powder versus composite films

FIG. 6. Plot of exponential time dependence of intensity. Units are in similar arbitrary intensity scale listed previously.

FIG. 7. Qualitative comparison of various emission peaks obtained through Gaussian deconvolution

FIG. 8. SEM micrograph of nanocomposite film. The two boxed areas were analyzed for composition and box 1 was found to have less zinc oxide than box 2. This suggests that the white agglomerations are not zinc oxide and that homogenous dispersion of the nanoparticles was achieved on a micron size scale.

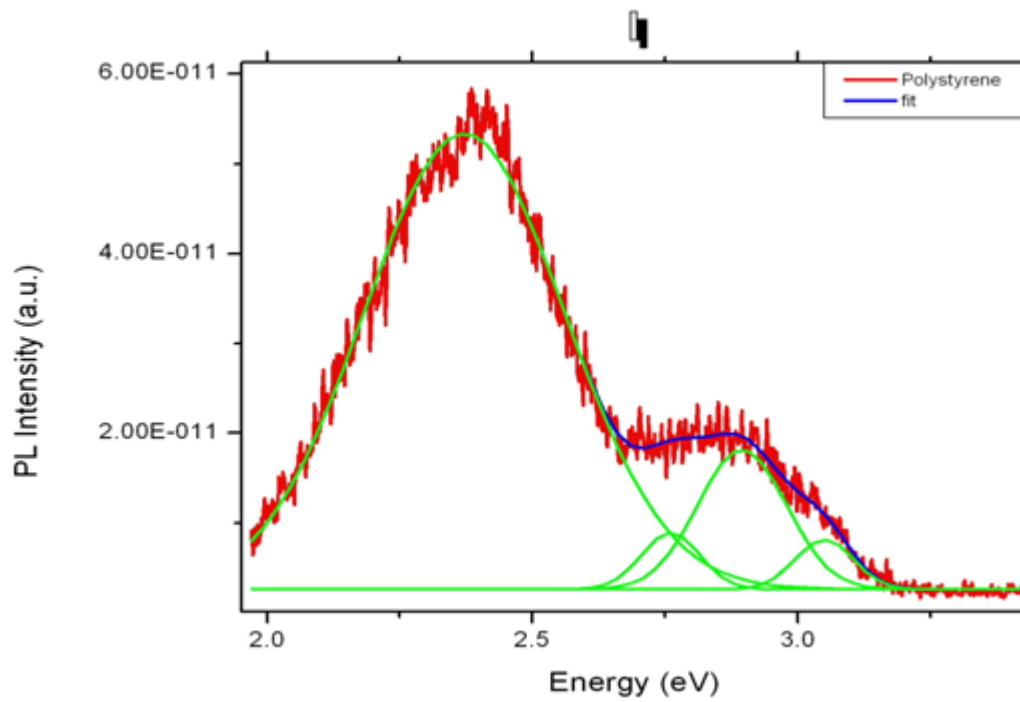


Figure 1

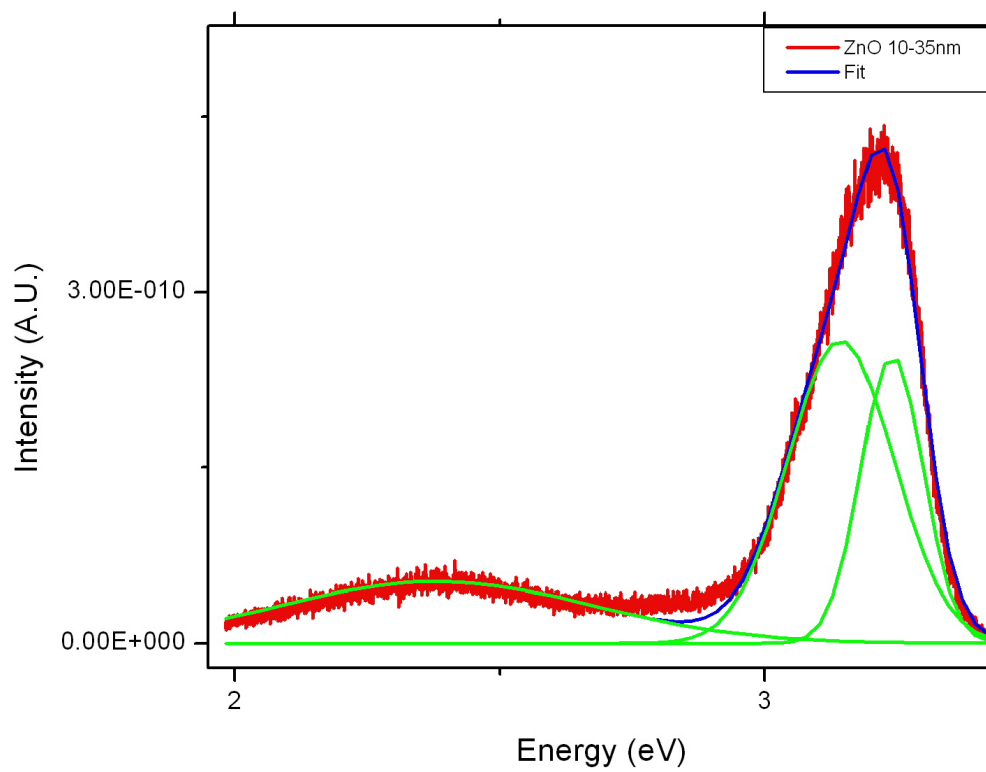


Figure 2

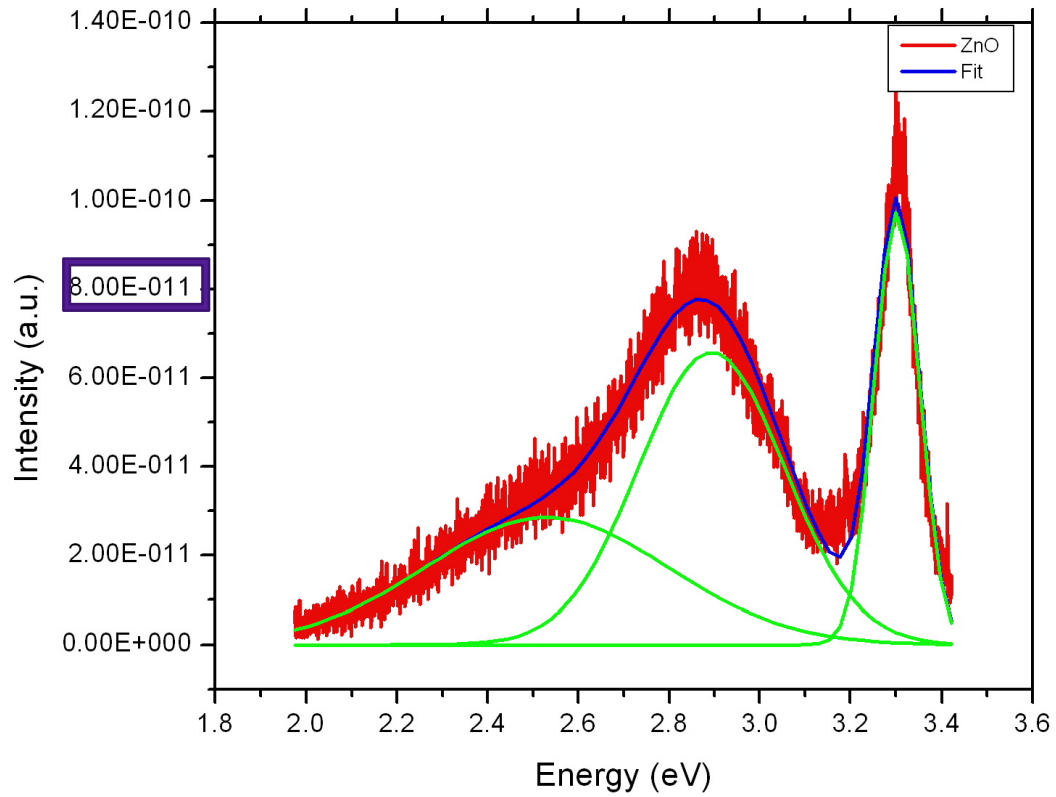


Figure 3

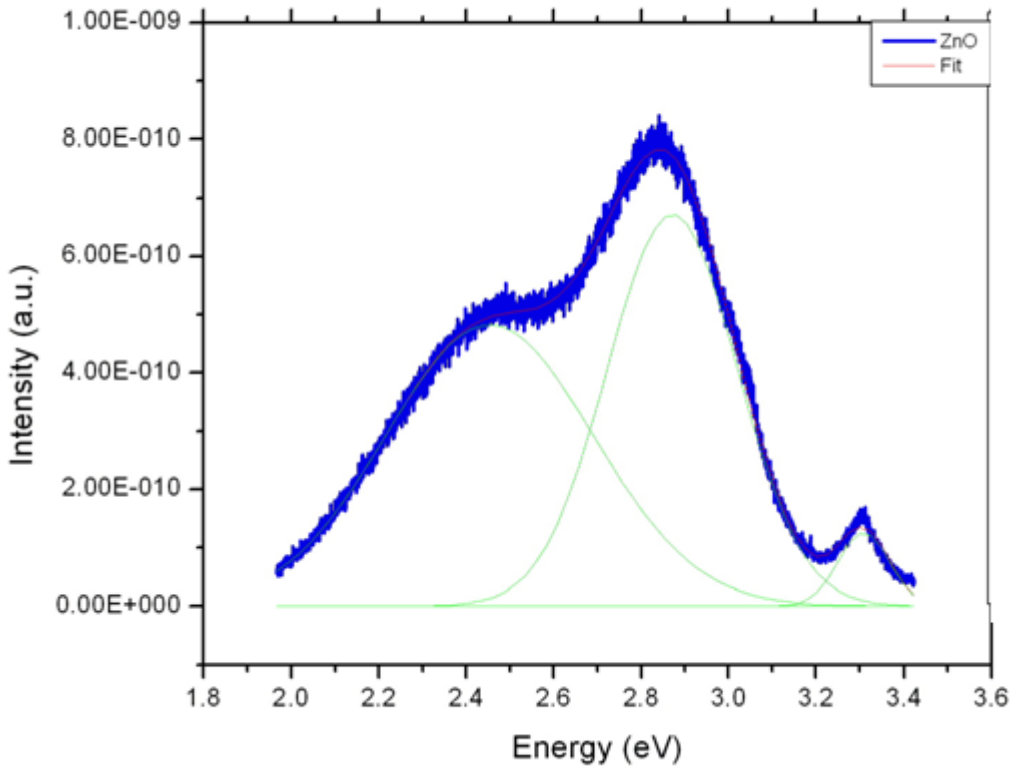


Figure 4

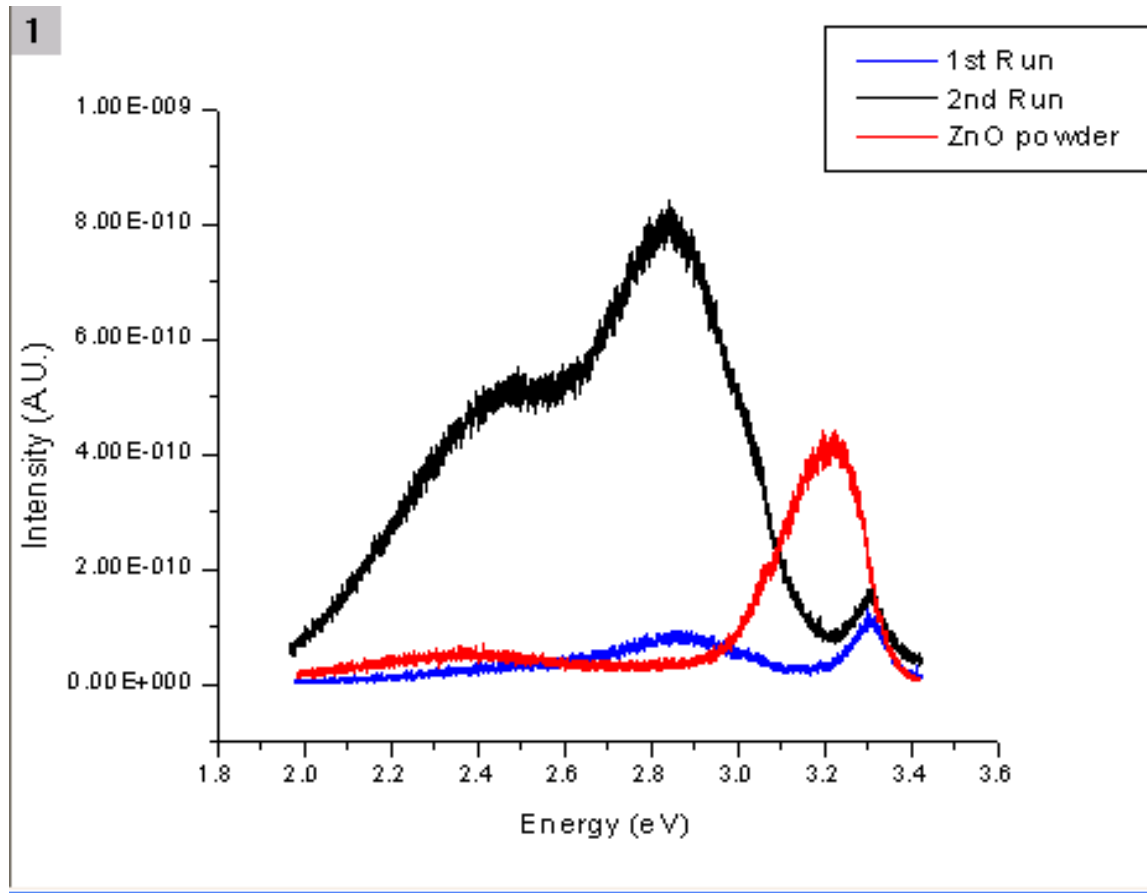


Figure 5

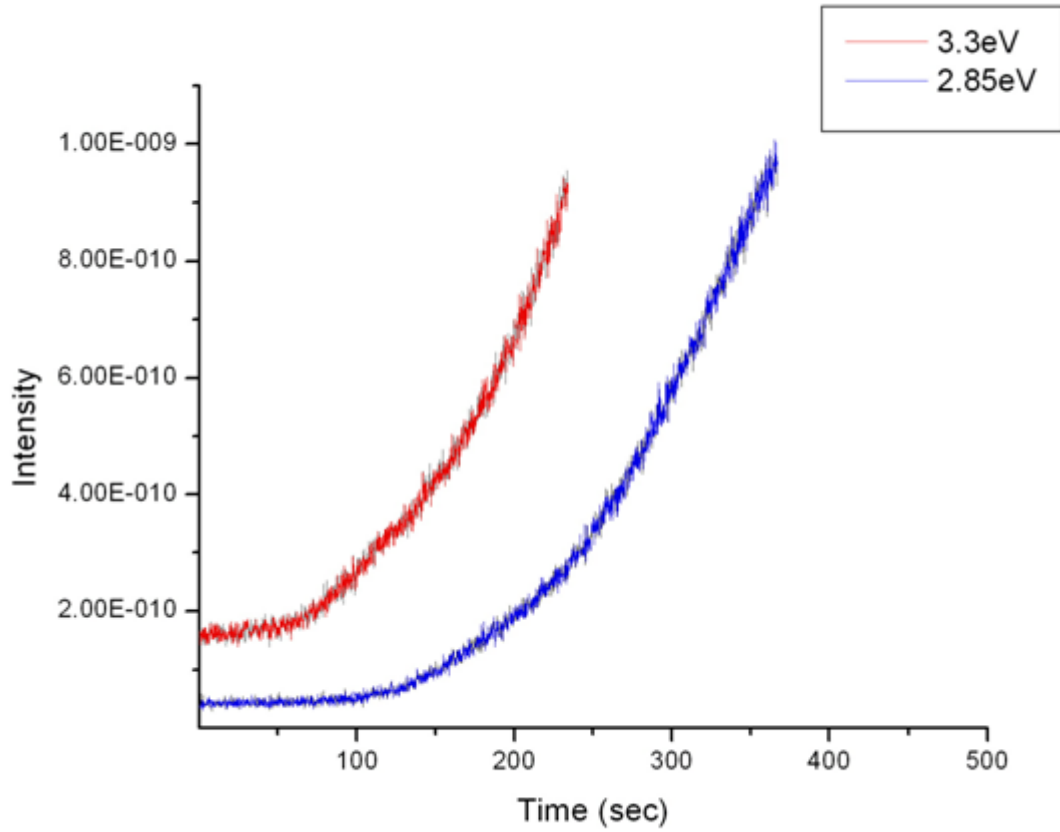


Figure 6

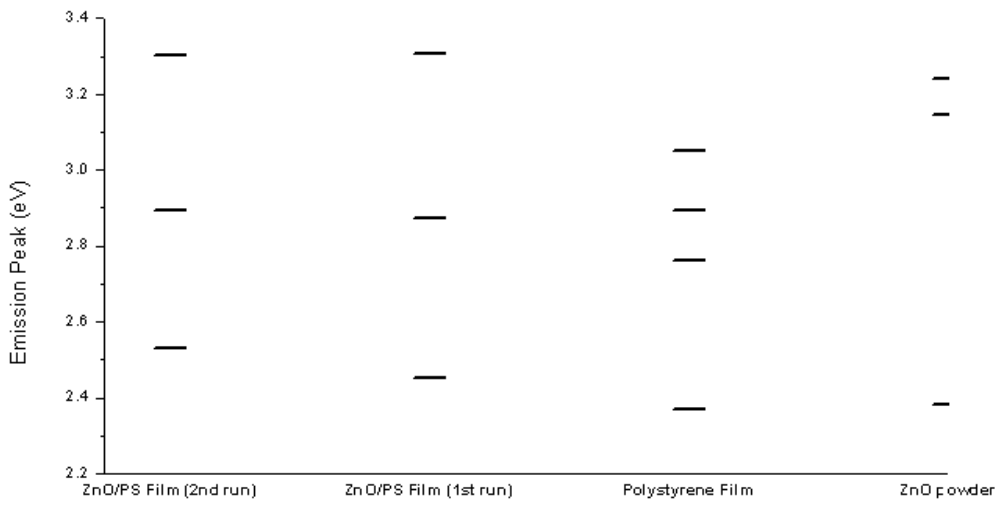


Figure 7

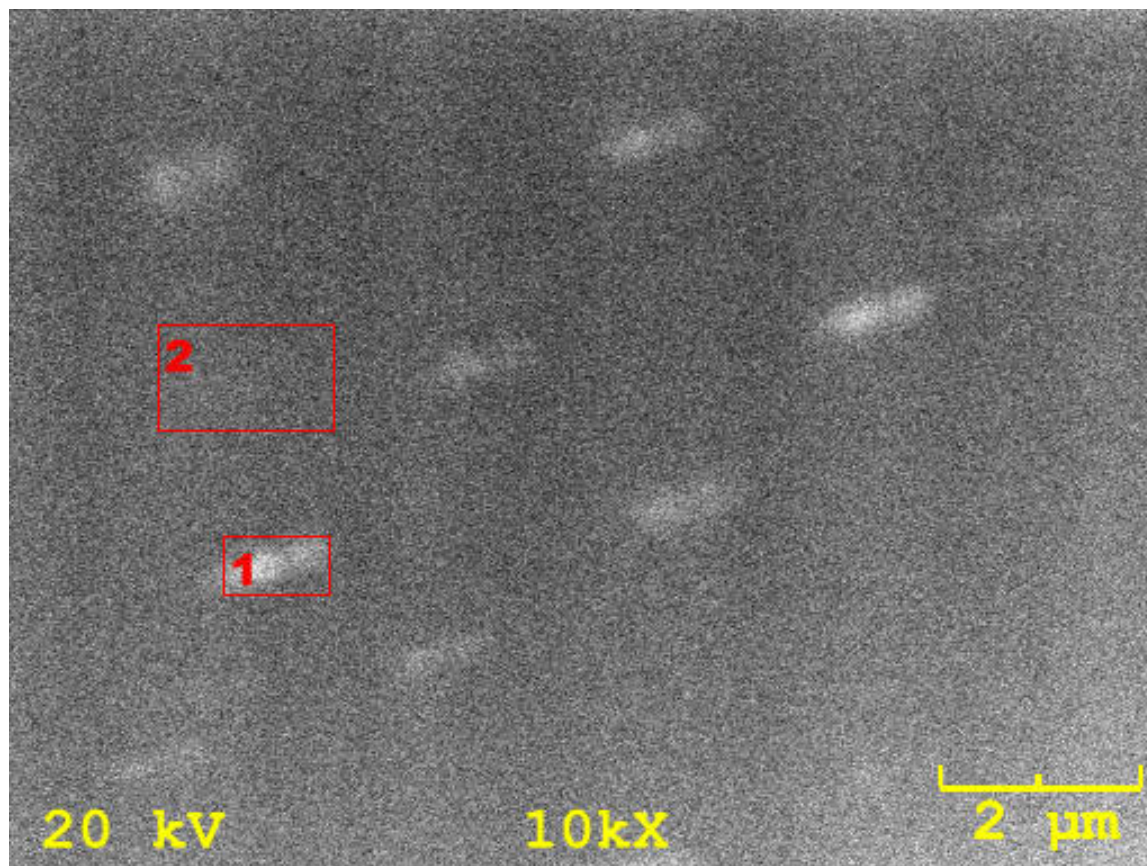


Figure 8